Molecular potentials and wave function mapping by high-resolution electron spectroscopy and ab initio calculations

ARTICLE *in* JOURNAL OF ELECTRON SPECTROSCOPY AND RELATED PHENOMENA · NOVEMBER 2013

Impact Factor: 1.44 · DOI: 10.1016/j.elspec.2013.11.003

2 AUTHORS:

Victor Kimberg
KTH Royal Institute of Technology
49 PUBLICATIONS **375** CITATIONS
SEE PROFILE

Catalin Miron
Horia Hulubei National Institute for R&D in …
158 PUBLICATIONS **1,520** CITATIONS
SEE PROFILE

Journal of Electron Spectroscopy and Related Phenomena xxx (2013) xxx–xxx

Contents lists available at ScienceDirect

Journal of Electron Spectroscopy and Related Phenomena

journal homepage: www.elsevier.com/locate/elspec

Molecular potentials and wave function mapping by high-resolution electron spectroscopy and *ab initio* calculations

Victor Kimberg[a], Catalin Miron[b,*]

[a] Max Planck Institute for the Physics of Complex Systems, Nöthnitzer Straße 38, 01187 Dresden, Germany
[b] Synchrotron SOLEIL, l'Orme des Merisiers, Saint-Aubin, BP 48, FR-91192 Gif-sur-Yvette Cedex, France

ARTICLE INFO

Article history:
Available online xxx

PACS:
33.80.−b
31.15.A
32.80.Aa
33.20.Rm

Keywords:
Inner-shell excitation
X-ray spectra
Resonant photoemission
Ab initio calculations
Vibrational wavefunction

ABSTRACT

The recent development of high brightness 3rd generation soft X-ray sources and high energy resolution electron spectrometers made it possible to accurately trace quantum phenomena associated to the vibrational dynamics in core-excited molecules. The present paper reviews the recent results on mapping of vibrational wave functions and molecular potentials based on electron spectroscopy. We discuss and compare the mapping phenomena in various systems, stressing the advantages of the resonant X-ray scattering for studying of the nuclear dynamics and spectroscopic constants of small molecules. The experimental results discussed in the paper are most often accompanied by state-of-the-art *ab initio* calculations allowing for a deeper understanding of the quantum effects. Besides its fundamental interest, the vibrational wave function mapping is shown to be useful for the analysis of core- and valence-excited molecular states based on the reflection principle.

1. Introduction

One of the fundamental concepts of modern chemical physics and quantum chemistry is the Born–Oppenheimer (BO) approximation, which allows considerable simplification of *ab initio* calculations and of the analysis of experimental molecular spectroscopy data. The BO approximation assumes that the total molecular wave function may be represented as a product of electronic and nuclear wave functions, thus decoupling the electronic and nuclear degrees of freedom. This wave function splitting allows one to employ a two-step approach. In the first step, one solves an electronic Schrödinger equation at fixed nuclei positions. The dependence of the electronic energy on nuclei's positions forms a potential energy surface or, in the one-dimensional case, a potential energy curve (PEC). In the second step, the nuclear dynamics is determined from the solution of the nuclear Schrödinger equation with a Hamiltonian which includes the nuclear kinetic energy and the electronic energy of a particular electronic state. This step may additionally involve separation of the vibrational, rotational and translational degrees of freedom. In the high-energy electron spectroscopy studies presented here, the translational and rotational motions have only minor effects observed in the spectral broadening of the lines [1,2], while the vibrational motion plays a crucial role in the spectra formation. The eigenfunctions of the vibrational Hamiltonian – the vibrational wave functions (VWFs) – and the PECs are well known quantum concepts, which are widely used in the interpretation of the modern ultrahigh resolution spectroscopic data tracing complex molecular dynamics. However, the question arises how these quantum concepts are related to the experimental observables, and if they can be mapped directly from the measurements?

The experimental scheme to address this question was proposed almost twenty years ago based on the theoretical prediction of the vibrational wave function mapping phenomena in the framework of the resonant X-ray scattering theory applied to the excitation/decay processes involving dissociative final states [3]. Indeed, the resonant scattering cross section was shown to be proportional to the square of the wave function of the vibrational sublevel involved in the scattering process [3–5], thus mapping its spatial distribution and the nodal structure according to the reflection principle [6]. In spite of the recent progress in vibrational motion tracking by pump-probe approaches using ultrashort laser pulses [7–11], only very few experimental studies have tried to address

* Corresponding author. Tel.: +33 169359605.
E-mail addresses: victor.kimberg@pks.mpi.de (V. Kimberg), miron@synchrotron-soleil.fr (C. Miron).

0368-2048/$ – see front matter © 2013 Elsevier B.V. All rights reserved.
http://dx.doi.org/10.1016/j.elspec.2013.11.003

this phenomenon in resonant photoemission (RPE) [12–18]. The main obstacles for the observation of the VWF mapping is a collective excitation of the vibrational sublevels when the photon bandwidth and lifetime broadening are broader than the vibrational quanta of the core-excited electronic state, as well as a high density of the final electronic states. To overcome this, one has to use an X-ray photon bandwidth smaller than the lifetime broadening (the so-called resonant Auger–Raman conditions [19,20]), and record ultrahigh resolution spectra allowing for an accurate state assignment. Such experimental conditions became recently available at the 3rd generation synchrotron X-ray radiation sources with the help of highly resolving instruments, and allowed for instance to establish new concepts [21] or to extract geometric information about core-excited states from RPE spectra of simple molecules [22,23]. Besides its fundamental interest, the experimental recording of the shapes of VWFs combined with state-of-the-art *ab initio* simulations allows analyzing the shapes of the core-excited and final-state potentials and deriving some important molecular parameters, such as the slope of the dissociative states PEC, the classical turning points of the bound PEC, their spectroscopic constants and the electronic transition energies.

In the present paper we summarize several recent results describing the PEC and VWF mapping in the framework of the high resolution electron spectroscopy. In particular, we focused on the observation of the VWF mapping in the RPE spectra of CO [12], N_2 [13,17,18], KF [15], BF_3 [14], and in the photoelectron-Auger electron coincidence spectrum of CH_4 [16]. The use of the recorded wavefunctions for the mapping of the potential energy curves of the core-excited [14] and final electronic states [14,16–18] are also discussed. In most of these cases the experimental results were analyzed with the help of *ab initio* simulations allowing to get a deeper insight into the studied quantum effects.

The paper is organized as follows. In Section 2, we give a brief theoretical description of the mapping phenomena manifestation on dissociative and bound molecular potentials. In Section 3, we summarize the experimental results showing the VWF mapping in the framework of the resonant photoelectron spectroscopy. In Section 4, we are discussing recently proposed techniques for molecular potentials reconstruction based on VWF reflection principle and *ab initio* calculations. We draw our conclusions in Section 5.

2. Vibrational wave function mapping phenomena in resonant X-ray scattering

The resonant photoemission process transfers the neutral molecule from its ground state to a number of excited electronic states of the singly ionized molecule with the emission of an electron of energy E from the valence orbitals. This process is enhanced when the photon frequency ω is tuned in resonance with a core-excited state, and the core electron is promoted to an unoccupied valence molecular orbital (see Fig. 1(a)). For an accurate simulation of the RPE spectra the time-dependent solution of the Schrödinger equation has to be employed [18]. However, the principle of VWF mapping phenomena can be explained based on the time-independent description of the scattering process [3]. Using the generalized Kramers–Heisenberg approach the RPE cross section reads in a general case [24] (in atomic units):

$$\sigma_0(E,\omega) \propto \sum_f |F_f|^2 \delta(\omega - E - \omega_{fg}), \quad F_f = \sum_i \frac{\langle \nu_f|Q|\nu_i\rangle\langle\nu_i|V|\nu_g\rangle}{\omega - \omega_{ig} + \imath\Gamma_i}. \tag{1}$$

Here we neglected the lifetime broadening of the final electronic state, which is much smaller than that of the intermediate (core-excited) state, Γ_i. δ is Dirac delta-function, V is the electronic matrix element of the dipole interaction of the incoming X-ray photons with the molecule, Q is the Coulomb interaction matrix element describing the Auger decay, $\omega_{jk} = \varepsilon_j - \varepsilon_k$ ($j, k = g, i, f$), ε_j and ν_j ($j = g, i, f$) are the eigenvalues and the eigenfuctions, respectively, of the nuclear Hamiltonian of the ground g, intermediate i, and final f electronic states.

In the case where the final electronic state is dissociative, the sum over final vibrational sublevels f in (1) should be replaced by the integration over energy of the final-state continuum, E_f. Let us linearly expand the final-state potential near the equilibrium position of the core-excited state R_0 as $E_f(R) = E_f(R_0) - (R - R_0)U_f$, where R is the internuclear distance and U_f is the interatomic force at R_0. In the limit of very short de Broglie wavelength, the continuum wave function of the final electronic state can be approximated by the Delta function at the classical turning point $\delta(R - R_t(E))$ [25]. This very simple model allows to see immediately the physics behinds the VWF mapping phenomena. Indeed, the integration over R and E_f are easily performed in that case, and the cross section (1) becomes:

$$\sigma_0(E,\omega) = \left| \sum_i A_i \frac{\nu_i(R_t)}{\omega - \omega_{ig} + \imath\Gamma_i} \right|^2, \quad A_i \propto VQ\langle\nu_i|\nu_g\rangle,$$
$$R_t(E) = R_0 + \frac{(\omega - E - \omega_{fg}(R_0))}{U_f}. \tag{2}$$

In (2) we assumed the validity of the Franck–Condon approximation, where the transition matrix elements V and Q are independent on R. Let us note that the calculations using a rather accurate approximation of the continuum wave functions by Airy functions [26] result in qualitatively the same equation for the shape of the RPE profile [3]. This can be understood from the simple consideration of Airy functions plotted in the central panel of Fig. 1(a). Indeed, the main contribution to the overlap integrals is given by the first main peak of the continuum function, while the rest vanishes due to its fast oscillatory behavior. In the case where photon bandwidth is smaller than the lifetime broadening of the core-excited state one can tune the X-ray energy in resonance with a single vibrational sublevel i_0 of the core-excited state. Eq. (2) clearly shows that in this case the RPE cross section

$$\sigma_0(E, \omega = \omega_{i_0 g}) \propto |\nu_{i_0}(R_t(E))|^2 \tag{3}$$

reflects the nodal structure of the core-excited state VWF: the zeros of the VWF are mapped one to one by the minima of the RPE profile. This phenomenon has a rather simple geometrical interpretation based on the reflection principle [6] as illustrated in Fig. 1(b). Although it is well known in the case of photodissociation dynamics [10,25], where the ground state vibrational wavefuctions are mapped, it was not observed until recently in the RPE case, which allows recording the VWF of the highly excited core-hole states with extremely short (few femtoseconds) lifetime. Let us note that reflection of the wavefunction is not exact but affected by the shape of the final-state potential. Apparently, the slope of the final-state PEC in the Franck-Condon region affects the energy interval between the spectral features reflecting the nodal structure of the core-excited state VWF. When the shape of the final-state potential is known, one can apply a reconstruction procedure in order to get the correct shape of the VWF.

Beyond the original prediction, the core-excited state VWF can be also mapped using bound final states. When the minimum of the potential is shifted toward larger bond lengths compared to the right classical turning point of the core-excited state wave packet the RPE cross section carries direct information about the nodal structure of the core-excited state VWF [18]. As illustrated in Fig. 1(b) the left classical turning point (short bond length) of the

Please cite this article in press as: V. Kimberg, C. Miron, Molecular potentials and wave function mapping by high-resolution electron spectroscopy and *ab initio* calculations, J. Electron Spectrosc. Relat. Phenom. (2013), http://dx.doi.org/10.1016/j.elspec.2013.11.003

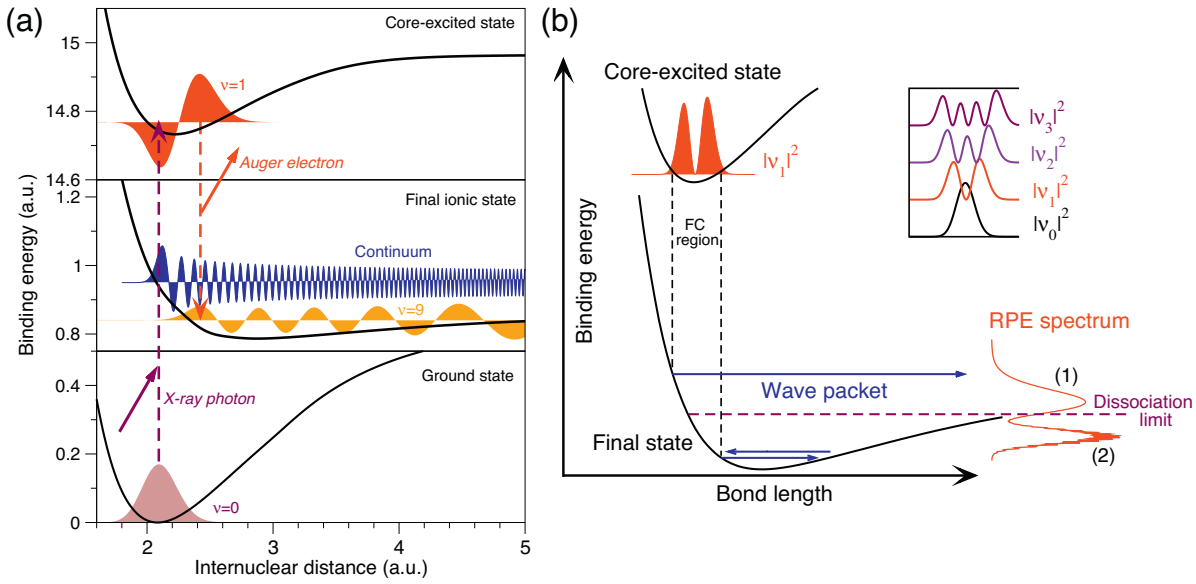

Fig. 1. (a) The scheme of the RPE process involving bound-continuum and bound-bound transitions. (b) Schematic representation of the VWF mapping on bound PEC [18]. The potential energy curves of the ground $^1\Sigma_g^+$, core-excited $^1\Pi_u$, and the final $1^2\Pi_g$ states of the nitrogen molecule, as well as the corresponding wave functions and the RPE spectrum are shown here.

wave packet in the core-excited state potential corresponds to a binding energy above the dissociation limit of the final state, which results in a broad dissociative-like spectral feature (1) as explained above. The right classical turning point (large bond length) corresponds to a binding energy below the dissociation limit of the final state: this part of the wave function generates a vibrational progression visible on top of the broad resonance (2) [27–30]. However, the envelope of the RPE profile maps the square of the core-excited state VWF with reasonably high accuracy. Indeed, the distribution of the Franck–Condon integrals $\langle \nu_f | \nu_{i_0} \rangle$ shows a maximum when the maximum of the core-excited VWF lies next to the left classical turning point of the final-state PEC (see Fig. 1(a)). A time-dependent analysis of the final-state wave-packet dynamics allows for a deeper insight in the formation of the RPE profile in the case of the VWF mapping on bound final states [18].

3. Vibrational wave function mapping in electron spectroscopy

The first tentative to record of the VWF mapping in the RPE framework was reported in [12], where the nodal structure of the vibrational wave functions of the C $1s \rightarrow 2\pi$ core-excited state of the CO molecule was observed using the valence-excited final states of the CO^+. However, the accurate VWF mapping in this case was rather difficult due to the strong overlap between many final electronic states in the so-called spectator band, which requires high spectral resolution to be able to extract the spectral characteristics related to a particular state. A similar observation in the RPE spectra of the N_2 molecule was reported in Ref. [13], where a nodal structure of the core-excited N $1s \rightarrow \pi^*$ state was partially reflected in the RPE spectrum of the $1^2\Pi_g$ final state of N_2^+. A very recent observation of the VWF mapping in the same system was much more successful thanks to the improved experimental conditions available nowadays [18]. In this experiment, the RPE spectra have been measured in a sub-lifetime regime (i.e. the X-ray bandwidth was much smaller ($\leq$20 meV) than the lifetime broadening of the core-excited state (115 ± 4 meV)), following selective N $1s \rightarrow \pi^*$ vibrational excitation, which allowed a given vibrational sublevel of the core-excited state to be selectively excited. Moreover, ultra-high spectral resolution combined with *ab initio* calculations made it possible to register the reflection of the core-excited VWF in the RPE spectra for several final states. Going beyond the original prediction related to dissociative final states [3], the vibrational wave function mapping was successfully carried out using bound final states of N_2^+ [18].

In Fig. 2, experimental RPE spectra are compared against full *ab initio* calculations taking into account twelve final excited

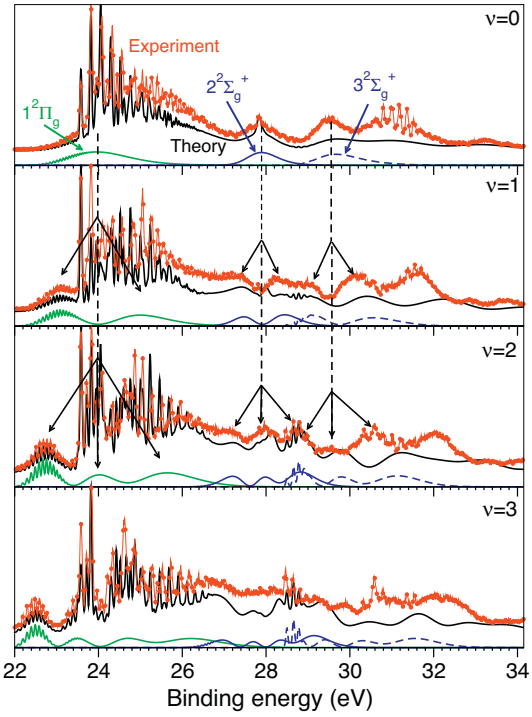

Fig. 2. Experimental (red circles) vs theoretical (black lines) RPE cross sections at the excitation energy tuned to the four lowest vibrational sublevels of the core-excited state $\nu = 0, 1, 2, 3$. The contributions from the three final states $1^2\Pi_g, 2,3^2\Sigma_g^+$ showing the VWF mapping are singled out and shown below the total theoretical spectrum. See [18] for details. (For interpretation of the references to color in this figure legend, the reader is referred to the web version of the article.)

Please cite this article in press as: V. Kimberg, C. Miron, Molecular potentials and wave function mapping by high-resolution electron spectroscopy and *ab initio* calculations, J. Electron Spectrosc. Relat. Phenom. (2013), http://dx.doi.org/10.1016/j.elspec.2013.11.003

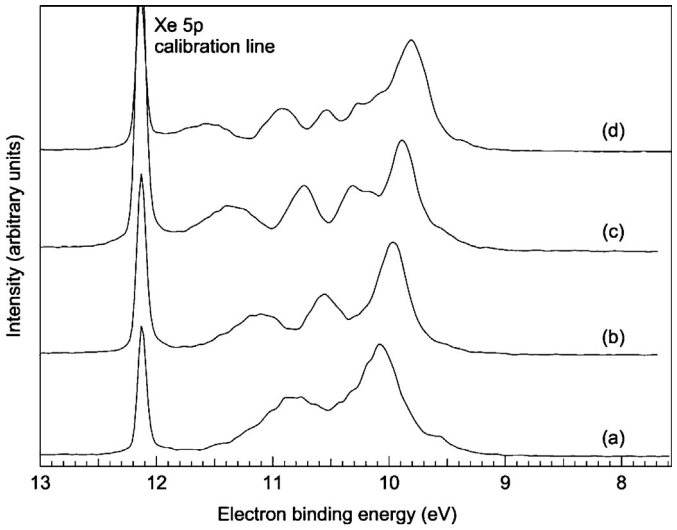

Fig. 3. Resonant photoemission spectra taken at photon energy tuned in resonance with several vibrational sublevels of the intermediate K3$p^{-1}\sigma$ ($^1\Pi$) core-excited state of KF: (a) $\nu=1$, (b) $\nu=2$, (c) $\nu=3$, and (d) $\nu=4$ (photon energies are 18.756 eV, 18.824 eV, 18.892 eV, and 18.973 eV, respectively). See [15] for details.

Reprinted figure with permission from [15]. Copyright (2009) by the American Physical Society.

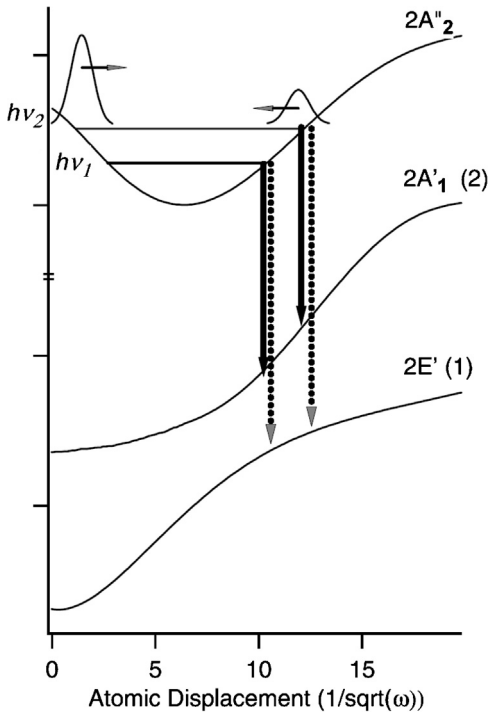

Fig. 4. Schematic diagram of the potential energy curves for the 2E′ and 2A_1' final ionic states and of the 2A_2'' core-excited state along the out-of-plane bending normal coordinate of BF_3. The decay from two different excitation energies is shown. The wave packet evolving from the inner to the outer turning point is represented on the resonant state potential energy curve. See [14] for details.

electronic states in this energy range. The theoretical RPE spectra for the three bound final states ($1^2\Pi_g$ and 2, $3^2\Sigma_g^+$) where the mapping phenomenon is most pronounced, are shown below the total spectra. Indeed, the envelopes of the RPE spectra mimic the corresponding profiles of the square of the excited wave functions $|\nu_i|^2$ ($i=0$, 1, 2, 3) (see inset in Fig. 1(b)) according to the reflection principle discussed above. Visual identification of the mapping effect in the experimental spectra is obvious for the two lowest core-excited vibrational substates $\nu=0$, 1. The broad peaks at 23.8, 27.9 and 29.6 eV ($\nu=0$) are split into two components in the $\nu=1$ RPE spectrum – 23.1 and 25.0 eV ($1^2\Pi_g$ state), 27.5 and 28.3 eV ($2^2\Sigma_g^+$), and 29.1 and 30.3 eV ($3^2\Sigma_g^+$) – reflecting the nodal structure of the $|\nu_1|^2$ function. Unfortunately, for higher excited vibrational sublevels the nodal structure is not directly visible in the region above 24 eV due to the high density of final states, and theoretical support becomes crucial for a thorough interpretation of the experimental data in relation to the mapping phenomenon.

A much clearer observation of the VWF mapping phenomenon is possible in the case where an isolated dissociative final state is available. This however is a rather rare situation for RPE in molecules. An isolated quasi-dissociative final state can be found in alkali halides monomers having rather elongated ionic bond length as compared to the covalent bonds. The VWF mapping was recently shown using the KF molecule [15]. Here the Auger decay following the excitation of various vibrational sublevels $\nu=1$, 2, 3, 4 of the intermediate K3$p^{-1}\sigma$ ($^1\Pi$) state results in a well resolved mapping of the core-excited VWF using the weakly bound final ionic state (see Fig. 3). Here some deviation from the mapping of the perfect nodal structure of an isolated VWF can be attributed to the lifetime vibrational interference (LVI) effect, the direct ionization channel contribution, as well as to weak contributions from other intermediate and final electronic states. Theoretical *ab initio* calculations show a rather good qualitative agreement with the experimental results [15]. The observation of the VWF mapping in this case also allowed to unambiguously identify the vibrational excitation in the core-excited state, which is difficult otherwise due to the overlap of several core-excited electronic states.

4. Mapping the molecular potentials based on the reflection principle

The VWFs, as eigenvectors of the nuclear Hamiltonian, can serve in general as unique fingerprints of a particular PEC. It looks rather tempting to reconstruct the PEC based on the observed VWF mapping. However, such reconstruction is not exact due to the approximate character of the reflection principle itself [6]. As it was recently shown with the help of *ab initio* calculations for the case of the X-ray Raman scattering in HCl [31], there is a slight deviation of the PEC reconstructed using the mapped VWF from the real one, and additional fitting of the potential parameters is usually needed. However, reflection of the nodal structure of the VWF allows to estimate with reasonable accuracy many important parameters of the core-excited and final ionic states, such as the classical turning points of the bound states, slopes of the dissociative states, transition energies and spectroscopic constants.

While the parallelism of the core-excited and final-states PEC has been discussed in O_2 based on the dispersion properties of RPE lines [32], the first attempt to use the VWF mapping phenomena in RPE for the reconstruction of the PEC properties in a polyatomic molecule was reported for BF_3 in Ref. [14]. In this study RPE was applied for the characterization of rather complex multi-mode potential energy surfaces of the core-excited state. The B $1s \rightarrow 2A_2''$ transition leads mainly to the excitation of the out-of-plane vibrational mode of BF_3. Tuning the photon energy through the absorption resonance results in a shift of the characteristic spectral features of the RPE profile, which was rationalized in the frame of the relative slopes of the PECs along the boron out-of-plane displacement coordinates. The principle of the potential reconstruction is illustrated in Fig. 4. The molecule experiences a conformation change from a planar conformation in the ground electronic state (D_{3h} point group) to a pyramidal one in the 2A_2'' core-excited state (C_{3v} point group) upon boron 1s electron

Please cite this article in press as: V. Kimberg, C. Miron, Molecular potentials and wave function mapping by high-resolution electron spectroscopy and *ab initio* calculations, J. Electron Spectrosc. Relat. Phenom. (2013), http://dx.doi.org/10.1016/j.elspec.2013.11.003

excitation. Such a change of the electronic structure induces a strong out-of-plane bending in the core-excited state which results in the ultrafast wave-packet propagation reaching the classical turning points of the core-excited potential. The core excitation followed by Auger decay promotes the molecule to a number of final singly-ionized states of a planar geometry. This allows to probe the out-of-plane bending mode in the intermediate and final states related to a dramatic geometry change. More specifically, the shift of the broad spectral features of the RPE spectra in the electron energy scale [14] related to the final state $2E'$ experiences a shift to a larger energy, since the slope of the final-state potential has a gentler slope as compared to the core-excited state potential around the classical turning point. The situation is opposite for the case of the $2A_1'$ state, where the RPE feature experiences a shift toward lower energies accordingly to the discussion above. This potential characterization method is relevant in numerous other cases as soon as a specific vibrational normal coordinate can be excited.

Using more complex schemes such as the coincidence techniques allows to extract information about the states not available from RPE measurements of the neutral molecules. A recent work reported photoelectron-Auger electron coincidence measurements in CH_4 [16]. The physical process consists of the photoionization of the C 1*s* electrons with an X-ray photon followed by the KVV Auger decay leading to doubly-ionized final states. The coincidence map here is formed by the photoelectron and Auger electron energy correlations. With the help of a theoretical deconvolution of the spectra, the authors showed in that case a possibility for the mapping of the core-ionized C $1s^{-1}$ VWFs. Moreover, the application of the reflection principle allowed to extract the parameters of the PECs of some final, doubly-ionized states of the molecule based on theoretical analysis. Assuming a harmonic potential for the core-ionized state and using an analytic expression for the wave function of the two lowest $\nu = 0, 1$ vibrational sublevels of the symmetric stretching mode, the slopes and the energies of the final dicationic states were obtained with the help of the reflection principle. The extracted values were compared against *ab initio* calculations and showed a relatively good agreement. The proposed method is rather general, but the provided analysis was very much limited by the statistics of the measurements. As suggested by the authors [16] the quality can be improved by using additional data for the coincidence with higher core-ionized vibrational sublevels, or by supplementary measurements of the CD_4 molecule.

An accurate PEC reconstruction for singly-ionized states was recently shown in the framework of the RPE spectroscopy in the case of N_2 [17]. The key idea of that study was to control the spatial distribution of the core-excited VWF by tuning the X-ray photon energy, which in turn allows to control the amount of vibrational energy excitation in the final states. The proposed approach is illustrated in Fig. 5 showing the reconstruction of the $1^2\Pi_g$ and $1^2\Delta_g$ PECs of N_2^+, where the later state was observed for the first time thanks to the proposed method. The ultrahigh resolution RPE spectra recorded on top of the first seven ($\nu = 0$–6) vibrational sublevels of the N $1s \rightarrow \pi^*$ core-excited state, were used for the potential reconstruction. The X-ray absorption peaks related to the $\nu = 5, 6$ sublevels have very weak oscillator strength, which results in a very low emission intensity of the resonant Auger electrons and the high statistics was only possible owing to the especially high photon flux available in the experiment [17,18]. The use of such highly excited vibrational sublevels is essential for the accurate potential reconstruction, since owing to the broad spatial distribution of their core-excited wave functions, only these states are able to populate the lowest vibrational substates in the $1^2\Pi_g$ and $1^2\Delta_g$ final electronic states (Fig. 5). The obtained vibrational progressions were used for the extraction of the harmonic frequency ω_e and anharmonicity $x_e\omega_e$ of the studied PECs, while the equilibrium distance was found by

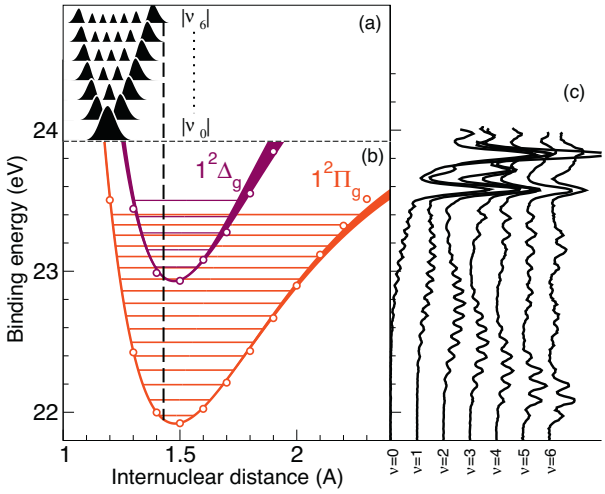

Fig. 5. Mapping of the N_2^+ PECs: (a) the seven lowest VWF of the core-excited state; (b) reconstructed molecular potentials (solid lines) compared against *ab initio* calculations (open circles); (c) the experimental RPE spectra are presented in relation to the reconstructed potentials. See [18] for details.

fitting the calculated Franck–Condon distribution. The extracted potentials show a very good agreement with the literature and the *ab initio* calculations. The method can be also extended to the study of the excited ionic states of larger species and transposed to neutral molecular states by detecting the radiative decay instead of RPE.

5. Conclusions

In the present article we reviewed the available experimental studies related to the mapping of the molecular potentials and vibrational wave functions using the high resolution resonant photoemission and related techniques. The results obtained by several independent research groups clearly confirm the possibility to observe these mapping phenomena based on transitions involving core-excited and core-ionized states of small molecules. The core-excited wave functions mapping was shown using both dissociative and bound final states. In the later case, the states with sufficiently elongated geometry are required, so that the equilibrium bond length is beyond the right classical turning point of the core-excited wave packet. These states usually lie in a region of high valence excitation in molecules where a high density of electronic states hinders the mapping phenomena to be clearly observed. A more distinct mapping is possible to observe on isolated low-lying final states of weakly bound systems, such as alkali halides or atomic dimers. In any case, high-resolution experimental data have to be accompanied by *ab initio* calculations for an accurate description of the mapping phenomena. Besides its general fundamental interest, the vibrational wave function mapping can be used for the analysis of molecular states. Based on the reflection principle some important properties and constants of the intermediate core-hole and final valence-hole potential energy curves can be extracted when the vibrational wave function mapping phenomenon is observable in the experiment. We discussed recent observations of the mapping phenomena in the resonant photoemission spectra of CO, N_2, KF, BF_3, and the photoelectron – Auger electron coincidence spectra of CH_4, as well as the successful extraction of the PEC parameters and excitation energies in the BF_3^*, BF_3^+, CH_4^{2+} and an accurate molecular potential reconstruction for the N_2^+ cation. All the discussed mapping techniques are rather general and can be successfully applied for the study of the neutral and ionic excited states of other small molecules in the framework of the resonant X-ray scattering.

Please cite this article in press as: V. Kimberg, C. Miron, Molecular potentials and wave function mapping by high-resolution electron spectroscopy and *ab initio* calculations, J. Electron Spectrosc. Relat. Phenom. (2013), http://dx.doi.org/10.1016/j.elspec.2013.11.003

References

[1] Y.-P. Sun, C.-K. Wang, F. Gel'mukhanov, Phys. Rev. A 82 (2010) 052506.
[2] T.D. Thomas, E. Kukk, K. Ueda, T. Ouchi, K. Sakai, T.X. Carroll, C. Nicolas, O. Travnikova, C. Miron, Phys. Rev. Lett. 106 (2011) 193009.
[3] F. Gel'mukhanov, H. Ågren, Phys. Rev. A 54 (1996) 379.
[4] Z.W. Gortel, R. Teshima, D. Menzel, Phys. Rev. A 58 (1998) 1225.
[5] N. Moiseyev, R. Santra, J. Zobeley, L.S. Cederbaum, J. Chem. Phys. 114 (2001) 7351.
[6] G. Herzberg, Spectra of Diatomic Molecules, van Nostrand Rein-hold, New York, 1950.
[7] S. Chelkowski, P.B. Corkum, A.D. Bandrauk, Phys. Rev. Lett. 82 (1999) 3416.
[8] S. De, I.A. Bocharova, M. Magrakvelidze, D. Ray, W. Cao, B. Bergues, U. Thumm, M.F. Kling, I.V. Litvinyuk, C.L. Cocke, Phys. Rev. A 82 (2010) 013408.
[9] D. Brinks, F.D. Stefani, F. Kulzer, R. Hildner, T.H. Taminiau, Y. Avlasevich, K. Müllen, N.F. van Hulst, Nature 465 (2010) 905.
[10] L.Ph.H. Schmidt, T. Jahnke, A. Czasch, M. Schöffler, H. Schmidt-Böcking, R. Dörner, Phys. Rev. Lett. 108 (2012) 073202.
[11] M. Magrakvelidze, O. Herrwerth, Y.H. Jiang, A. Rudenko, M. Kurka, L. Foucar, K.U. Kühnel, M. Kübel, Nora G. Johnson, C.D. Schröter, S. Düsterer, R. Treusch, M. Lezius, I. Ben-Itzhak, R. Moshammer, J. Ullrich, M.F. Kling, U. Thumm, Phys. Rev. A 86 (2012) 013415.
[12] M.N. Piancastelli, M. Neeb, A. Kivimäki, B. Kempgens, H.M. Köppe, K. Marier, A.M. Bradshaw, R.F. Fink, J. Phys. B: At. Mol. Opt. Phys. 30 (1997) 5677.
[13] M.-N. Piancastelli, A. Kivimäki, B. Kempgens, M. Neeb, K. Maier, U. Hergenhahn, A. Rüdel, A.M. Bradshaw, J. Electron Spectrosc. Relat. Phenom. 98-99 (1999) 111.
[14] C. Miron, R. Feifel, O. Björneholm, S. Svensson, A. Naves de Brito, S.L. Sorensen, M.N. Piancastelli, M. Simon, P. Morin, Chem. Phys. Lett. 359 (2002) 48.
[15] M. Patanen, S. Urpelainen, M. Huttula, R. Sankari, V. Kisand, E. Nõmmiste, E. Kukk, H. Aksela, S. Aksela, Phys. Rev. A 80 (2009) 013414.
[16] R. Püttner, T. Arion, M. Förstel, T. Lischke, M. Mucke, V. Sekushin, G. Kaindl, A.M. Bradshaw, U. Hergenhahn, Phys. Rev. A 83 (2011) 043404.
[17] C. Miron, C. Nicolas, O. Travnikova, P. Morin, Y. Sun, F. Gel'mukhanov, N. Kosugi, V. Kimberg, Nat. Phys. 8 (2012) 135.
[18] V. Kimberg, A. Lindblad, J. Söderström, O. Travnikova, C. Nicolas, Y.P. Sun, F. Gel'mukhanov, N. Kosugi, C. Miron, Phys. Rev. X 3 (2013) 011017.
[19] A. Kivimäki, A. Naves de Brito, S. Aksela, H. Aksela, O.-P. Sairanen, A. Ausmees, S.J. Osborne, L.B. Dantas, S. Svensson, Phys. Rev. Lett. 71 (1993) 4307–4310.
[20] G. Armen, H. Aksela, T. Åberg, S. Aksela, J. Phys. B: At. Mol. Opt. Phys. 33 (2000) R49.
[21] R. Feifel, A. Baev, F. Gel'mukhanov, H. Ågren, M.N. Piancastelli, M. Andersson, G. Öhrwall, C. Miron, M. Meyer, S.L. Sorensen, A. Naves de Brito, O. Björneholm, L. Karlsson, S. Svensson, Phys. Rev. A 69 (2004) 022707.
[22] R. Feifel, F. Gel'mukhanov, A. Baev, H. Ågren, M.N. Piancastelli, M. Bässler, C. Miron, S.L. Sorensen, A. Naves de Brito, O. Björneholm, L. Karlsson, S. Svensson, Phys. Rev. Lett. 89 (2002) 103002.
[23] A. Baev, R. Feifel, F. Gel'mukhanov, H. Ågren, M.N. Piancastelli, M. Bässler, C. Miron, S.L. Sorensen, A. Naves de Brito, O. Björneholm, L. Karlsson, S. Svensson, Phys. Rev. A 67 (2003) 022713.
[24] F. Gel'mukhanov, H. Ågren, Phys. Rep. 312 (1999) 87.
[25] R. Schinke, Photodissociation Dynamics, Cambridge University Press, New York, 1993.
[26] K.F. Freed, Y.B. Band, Product energy distributions in the dissociation of polyatomic molecules, in: E.G. Lim (Ed.), Excited States, 3rd ed., Academic Press, New York, 1977.
[27] M. Neeb, J.-E. Rubensson, M. Biermann, W. Eberhardt, K.J. Randall, J. Feldhaus, A.L.D. Kilcoyne, A.M. Bradshaw, Z. Xu, P.D. Johnson, Y. Ma, Chem. Phys. Lett. 212 (1993) 205.
[28] M. Neeb, J.-E. Rubensson, M. Biermann, W. Eberhardt, J. Electron Spectrosc. Relat. Phenom. 67 (1994) 261.
[29] J.-E. Rubensson, M. Neeb, M. Biermann, Z. Xu, W. Eberhardt, J. Chem. Phys. 99 (1993) 1633.
[30] W. Eberhardt, J.-E. Rubensson, K.J. Randall, J. Feldhaus, A.L.D. Kilcoyne, A.M. Bradshaw, Z. Xu, P.D. Johnson, Y. Ma, Phys. Scr. T 41 (1992) 143.
[31] S. Carniato, R. Taïeb, R. Guillemin, L. Journel, M. Simon, F. Gel'mukhanov, Chem. Phys. Lett. 439 (2007) 402.
[32] S.L. Sorensen, R. Fink, R. Feifel, M.N. Piancastelli, M. Bässler, C. Miron, H. Wang, I. Hjelte, O. Björneholm, S. Svensson, Phys. Rev. A 64 (2001) 012719.

Please cite this article in press as: V. Kimberg, C. Miron, Molecular potentials and wave function mapping by high-resolution electron spectroscopy and *ab initio* calculations, J. Electron Spectrosc. Relat. Phenom. (2013), http://dx.doi.org/10.1016/j.elspec.2013.11.003